applied microbiology

Article

Use of Integrated Core Proteomics, Immuno-Informatics, and In Silico Approaches to Design a Multiepitope Vaccine against Zoonotic Pathogen *Edwardsiella tarda*

Sk Injamamul Islam [1,2,*], Sarower Mahfuj [1,2], Md Jakiul Islam [3], Moslema Jahan Mou [4] and Saloa Sanjida [5]

[1] Department of Fisheries and Marine Bioscience, Faculty of Biological Science, Jashore University of Science and Technology, Jashore 7408, Bangladesh; 6378807231@student.chula.ac.th
[2] Center of Excellence in Fish Infectious Diseases (CE FID), Department of Veterinary Microbiology, Faculty of Veterinary Science, Chulalongkorn University, Bangkok 10330, Thailand
[3] Faculty of Biology and Chemistry (FB 02), University of Bremen, 28359 Bremen, Germany; mdjislam@uni-bremen.de
[4] Department of Genetic Engineering and Biotechnology, Faculty of Earth and Life Science, University of Rajshahi, Rajshahi 6205, Bangladesh; moslemajahanmou@gmail.com
[5] Department of Environmental Science and Technology, Faculty of Applied Science, Jashore University of Science and Technology, Jashore 7408, Bangladesh; saloaest12.just@gmail.com
* Correspondence: injamamulislam017@gmail.com

Abstract: Multidrug-resistant *Edwardsiella tarda* has been reported as the main causative agent for massive fish mortality. The pathogen is well-known for causing hemorrhagic septicemia in fish and has been linked to gastrointestinal infections in humans. Formalin-inactivated *Edwardsiella* vaccination has previously been found to be ineffective in aquaculture species. Therefore, based on *E. tarda*'s integrated core complete sequenced genomes, the study aimed to design a subunit vaccine based on T and B cell epitopes employing immunoinformatics approach. Initially, the top immunodominant and antigenic epitopes were predicted from the core complete sequenced genomes of the *E. tarda* genome and designed the vaccine by using linkers and adjuvant. In addition, vaccine 3D structure was predicted followed by refinement, and molecular docking was performed for the analysis of interacting residues between vaccines with TLR5, MHC-I, and MHC-II, respectively. The final vaccine constructs demonstrated strong hydrogen bond interactions. Molecular dynamic simulation of vaccine-TLR5 receptor complex showed a stable structural binding and compactness. Furthermore, *E. coli* used as a model organism for codon optimization proved optimal GC content and CAI value, which were subsequently cloned in vector pET2+ (a). Overall, the findings of the study imply that the designed epitope vaccine might be a good option for prophylaxis for *E. tarda*.

Keywords: *Edwardsiella tarda*; zoonosis; immunoinformatics; epitopes; vaccine

Citation: Islam, S.I.; Mahfuj, S.; Islam, M.J.; Mou, M.J.; Sanjida, S. Use of Integrated Core Proteomics, Immuno-Informatics, and In Silico Approaches to Design a Multiepitope Vaccine against Zoonotic Pathogen *Edwardsiella tarda*. *Appl. Microbiol.* **2022**, *2*, 414–437. https://doi.org/10.3390/applmicrobiol2020031

Academic Editor: Hosni M. Hassan

Received: 3 June 2022
Accepted: 15 June 2022
Published: 18 June 2022

1. Introduction

Edwardsiella tarda (*E. tarda*) is found in a wide range of hosts, namely, humans and animals including fish. *E. tarda* is a widespread organism reported to have been found at fish farms in the United States, South America, Asia, Middle-east, and Africa. It has also been found in wild fish from Canada, the United States, and Australia. It is worth noting that *E. tarda* infections cause the most common bacterial infection and illness in both freshwater and marine water fish and result in massive mortality [1]. *E. tarda* causes both Edwardsiellosis and systemic hemorrhagic septicemia in fish, which is marked by internal abscesses and widespread skin inflammation and discoloration [2]. Japanese eels, channel catfish, chinook salmon, rainbow trout, Nile tilapia, siamese fighting fish, red sea bream, turbot, angelfish, crimson, European seabass, and black tetra are all susceptible to this bacterium [3]. The massive fish mortality in aquaculture caused by this pathogen causes economic losses in the US, Japan, and India [4]. Moreover, this bacterium can cause infection

in humans and results in dysentery, gastroenteritis, typhoid-like illness, peritonitis with sepsis, and sometimes even death [5]. In addition to invasion capability, *E. tarda* releases siderophores that induce inflammation and abnormal host cell function, as well as biofilm formation [6–8]. Every year on aquaculture farms, a huge amount of antibiotics is used for both treatment and prophylaxis measures. However, this approach has exacerbated the threat posed by drug-resistant bacteria, such as *E. tarda*, to the aquaculture industry and public health [9,10]. Virulent *E. tarda*, isolated from Japanese flounder infected with Edwardsiellosis, has demonstrated high resistance to kanamycin, tetracycline, ampicillin, and streptomycin. It also seems to be resistant to many other antibiotics often used in farmed fish [11]. Tetracycline resistance, for example, is mostly mediated by proton-dependent efflux pumps found in Gram-negative bacteria, as well as ribosomal proteins of Gram-positive bacteria [12]. Antibiotic resistance is a complex phenomenon involving complex networks of genes, proteins, and biological processes [13]. Such Gram-negative bacteria, e.g., *E. tarda*, can be found in both freshwater and marine environments. Because of the presence of unique fimbriae, *E. tarda* has a strong attraction to red blood cells and exhibits hemagglutination characteristics [14].

Cytotoxic T lymphocyte epitopes of fish were discovered from in vivo experiments and a peptide database of the overlapping pathogens [15] and CD4+ T cell epitopes were detected in a diverse range of species [16,17]. Fish possess immunoglobulins, major histocompatibility complexes, T-cell receptors, and lymphocytes that can elicit specific immune responses against a wide range of antigens, which are similar to those produced by B and T cells [17]. Vaccines boost the immune system to produce a response against a potentially lethal foreign pathogen to infiltrate the particles, reduce their toxic effects, or initiate the assassination of the pathogen. However, vaccination can be used as prophylaxis to prevent future outbreaks of pathogens (e.g., viruses and bacteria) [18].

The in silico design of multiepitope vaccines allows for the rapid identification of safe, effective, uncomplicated, inexpensive, and predictable immune responses to the directed antigen(s). Because of improper knowledge of the distinctions between human leukocyte (HLA) antigen and MHC-I and MHC-II, the in silico technique in fish has yet to be developed [19,20]. However, current fish genomics research has provided enough data to use in silico methodologies and procedures [21–23]. MHC-I and MHC-II molecules, which are vital for triggering immunological responses to infections, have been discovered in chord and tilapia, for example [21]. MHC class I against class II, and polymorphism classical versus nonpolymorphic nonclassical, are the primary patterns of MHC variation in fish, which are identical to mammals. Furthermore, the pattern of MHC-I and MHC-II in fish and polymorphic classical versus non-polymorphic classical in mammals is identical [21]. Thus, the peptide with excellent HLA-A*0201, HLA-B*3501, and HLA-B*3508 binding capabilities might be used as effective vaccines against specific fish illnesses [19,24]. Moreover, the MHC-II DAA and DAB allele has already been observed in Rainbow trout. In addition, the immunoinformatic approach was proved effective for epitope (T-cell and B-cell) prediction in fish (essential to develop vaccine subunit) and showed strong reactivity in the presence of *Vibrio harveyi, Streptococcus agalactiae*, marine birna virus, and *Flavobacterium columnari* separately [25–29]. The advantage of the sub-unit vaccine is the zero risk of host or non-target species pathogenicity because this type of vaccine cannot multiply [30]. These types of vaccines are highly effective vaccines and can target specific microbiological determination of their immune responses, allow for non-natural substances to be added, and can be kept frozen for non-refrigerated shipping and storage. Therefore, the application of the subunit vaccine can boost fish immune responses by the peptide sequences. They cannot be altered or reverted since they are synthetic, and they are not contaminated by toxins and pathogens. Moreover, bringing desired change(s) in the peptide structure could improve stability and reduce undesirable side effects of the target vaccine subunit. Researchers predict that computer-assisted solutions will become increasingly effective in managing fish infections and diseases in the coming years [31,32]. Therefore, the primary

goal of this study was to identify epitopes from the most effective antigenic proteins for fighting *E. tarda* infection in fish.

2. Methods and Materials

2.1. E. tarda Core Proteome Identification

The architectural diagram of the methodology of this study is given in Figure 1. An analysis of the core complete sequenced genomes of the *E. tarda* genomes with a Perl script was carried out by downloading all 18 genome sequences from the NCBI database [33]. Using USEARCH, the proteomes were clustered, and proteins with less than 50% sequence identity were excluded from the analysis. Clustered sequences have been checked for protein presence or absence in all input genomic sequences. Finally, all the protein sequences from the core proteome analysis were considered for the vaccine construction. These conserved sequences are appealing when looking for possibilities for broad-spectrum vaccine development [34].

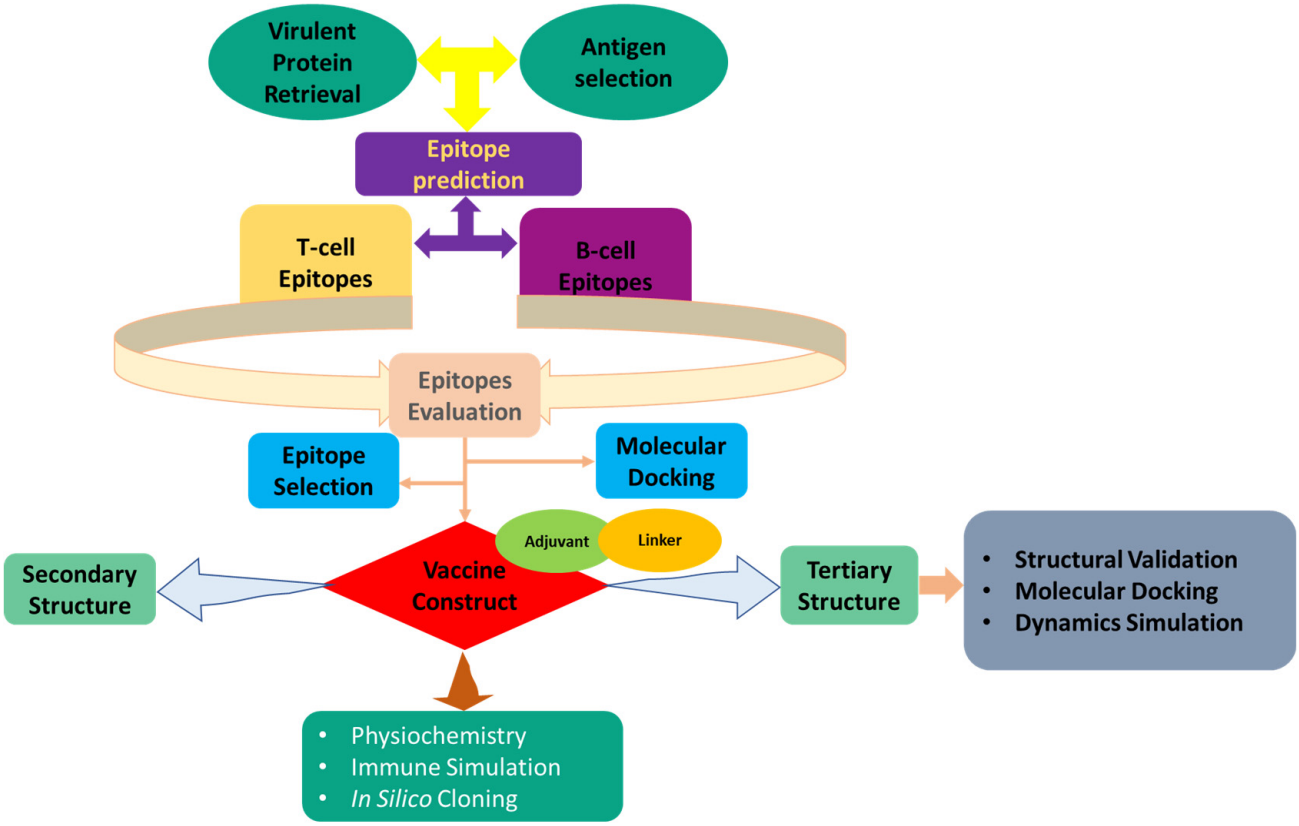

Figure 1. Architectural flowchart for vaccine subunit development.

2.2. Subtractive Proteomics and Approach

To discover novel vaccine candidates, subtractive proteome analysis is performed on the core proteome. The initial step in subtractive proteomics is to remove paralogue sequences. In the cluster database at high identity with tolerance (CD-HIT), nucleotide or protein sequences are compared and grouped to reduce duplicates and improve sequence analysis performance with minimal redundancy. CD-HIT is largely recognized as the most often utilized application for decreasing sequence mismatch. In this scenario, the CD-HIT server was used to screen the whole core proteome at an 80% threshold level. It ensures in reduction of repetition by adhering to a user-defined sequence identity threshold [35]. Using the CD-HIT proteins as a starting point, BlastP was used to search for non-homologous *E. tarda* proteins against a non-redundant database. BlastP (Protein-Protein BLAST) identifies the most similar protein sequences from different protein databases by comparing

the query protein with the database specified by the user [36]. Proteins were considered non-homologous if the query coverage was higher than 70% and the identity was greater than 30%. When generating vaccine candidates, it is crucial to understand the mechanism of a certain protein. Subcellular localization predictions are an effective and efficient way of determining the function of a protein. Additionally, studies have shown that since proteins are found in various locations, localization is an important factor in designing vaccine candidates. Thus, a CELLO server was used to predict non-homologous protein subcellular location. The CELLO can screen the subcellular localization of proteins using a multi-class SVM-based classification system [37]. It is important to understand virulent proteins because they are important in the etiology of many diseases. Proteins with non-homologous sequences were screened for virulence using the VFDB (Virulence Factor Database) proteins with a non-homologous sequence were subjected to VFDB (Virulence Factor Database) to be identified as virulent [38]. A homolog with a bit score >100 and an identity >30% for *E. tarda* pathogen was considered virulent. Transmembrane helices were determined using the TMHMM (Transmembrane Helices; Hidden Markov Model) server. TMHMM is a software that checks for transmembrane helices in proteins [39]. Multiple transmembrane helices proteins were excluded from the study due to their difficulty in producing, refining, and cloning and they are inappropriate for vaccine development [40]. In this research, the leading antigenic proteins containing transmembrane helices 0 or 1 were selected for vaccine construction. Eventually, Vaxijen Server 2.0 was used to predict the antigenicity score of all the selected pathogenic proteins [41]. Antigenic proteins with antigenicity scores greater than 0.5 were designated virulent proteins, and the antigenic proteins with the highest antigenicity ratings were chosen as potential vaccination candidates. Apart from that, the AllerTOP server evaluated the proteins' allergenic nature, and the Protparam program was used to determine their molecular features [42,43].

2.3. Epitopes Prediction

2.3.1. T-Cell Epitope Prediction

The CTLs are one type of immune cell that has the potential to damage completely infected and infectious cells [44]. They enter the cell instantly and participate in the host's defensive reaction. This study employed two T-cell epitope prediction servers to find the best antigenic, immunogenic, non-toxic, and non-allergenic epitopes. To anticipate T-cell epitopes, the sequences of the selected proteins were first input into the CTLPred server [45]. CTLPred used artificial neural networks (ANN) and stabilized matrix methods (SMM) in order to predict the ability of peptides to bind to the MHC molecules. Epitopes in this server were anticipated based on previously known alleles in vertebrates. Secondly, the Vaxitop (https://www.violinet.org/vaxign/vaxitop, accessed on 27 April 2022) server was used to select the top T-cell epitopes. Vaxitop predicted the epitopes of the principle of reverse vaccinology [46]. The anticipated epitopes were then evaluated further utilizing the VaxiJen v2.0 [41], MHC class I immunogenicity [47], ToxinPred [48], and AllerTop v2.0 [49] servers. The predictions were all done using the default parameters of the servers.

2.3.2. Epitopes of Linear B-Lymphocytes: Prediction and Evaluation

B-cells are composed of amino acid groups that attach to antibodies generated by the immune system and activate them to combat diseases [50]. B-cell epitopes are necessary to enhance humoral or antibody-mediated immunity. Thus, the iBCE-EL server was used with default parameters to predict the linear B-lymphocyte (LBL) epitopes [51]. VaxiJen v2.0, AllerTop v2.0, and ToxinPred v2.0 servers were applied to select the best antigenic, non-allergic, and non-toxic LBL epitopes, respectively.

2.4. Modeling of Peptides and Molecular Docking

The T-cell epitopes were simulated using the PEP-FOLD v3.0 server. To achieve this, 200 simulations of the sOPEP sorting algorithm were used [52]. HLA-A*0201, HLA-B*3501, and HLA-B*3508 and DAB1*07:01, DAB1*15:01, and DAA2*01:01, which are commonly

found alleles in fish, were chosen for selected T-cell epitopes, based on HLA binding allele analysis by epitope. The structures of HLA alleles were obtained from the Protein Data Bank (PDB) [53] and then processed with BIOVIA Discovery Studio 2017. An AutoDock grid box was constructed around each HLA allele's active site for molecular docking using the AutoDock program. Molecular docking between epitopes and related HLA alleles was also performed using the AutoDock Vina program [54]. As a positive control, appropriate co-crystal ligands were used to assess epitope binding efficacy. The docked complex's binding residues were evaluated by BIOVIA Discovery Studio 2017 and PBDSum.

2.5. Development of a Multi-Epitope Vaccine

The final vaccine was developed with the chosen epitopes (CTL and LBL) to enhance the immunogenicity, combining them with the appropriate adjuvants (50S ribosomal protein L7/L12) (NCBI ID: P9WHE3) and linkers. Because glycoproteins recognize TLR5, and adjuvants are required to overcome translation and synthesis restrictions, the adjuvant utilized here was a TLR5 agonist [55]. Attaching the adjuvant to the vaccine front was done by using the EAAAK bi-functional linker, throughout a broad range of peptide lengths, capable of breaking separate two b domains with weakly interlocking connections. AAY linkers interfaced with the chosen 9-mer sequence of CTL epitope, while GPGPG linkers interfaced with the 15-mer sequence of CTL epitope, and KK linkers interfaced with the LBL [50,56]. As a proteasome cleavage site, the selected linkers can be exploited to alter protein stability and immunogenicity, as well as to enhance epitope presentation [57].

2.6. Evaluation of Design Vaccine Characteristics

The essential features of a protein are described by its physiochemistry. ProtParam predicted the vaccine's physicochemical properties to make sense of its essence [58]. For the evaluation of immunological parameters, we used the VaxiJen v2.0 server, MHC-I immunogenicity server, AllerTop server, and SOLpro server.

2.7. 2D Structural Features Prediction

The SOPMA and PSIPRED v4.0 servers examined the designed vaccine's 2D structural properties [59] with default parameters. In SOPMA, over 80% of predictions are accurate [60]. Moreover, the design vaccine composition quality was analyzed by extracting 2D structural parameters

2.8. Validation and Homology Modeling of Vaccine 3D Structure

The complete vaccine sequence was uploaded to the RaptorX server. RaptorX uses a cutting-edge algorithm and a three-dimensional structure to compute the most precise structure and activity of a protein [61]. This online tool can forecast and calculate the value of the TM-score, C-score, RMSD, and the top five models of a certain amino acid sequence. The C-score value was used to choose the resulting 3D structure, which was stored as a PDB file. This server value runs from −5 to 2, with a higher number suggesting a more secure 3D structure. For vaccine structure refining, the determined 3D structure was transmitted to the GalaxyRefine online web-based tool. This webserver was operated using the CASP10 refining technique [62]. The most energy-efficient structure was chosen based on the revised structure's lowest and greatest RMSD ratings. The improved and found structure was shown using PyMOL v2.3.4 [63]. An analysis of the final 3D structure was conducted using the Ramachandran plot score and Z-score value, which provide information about standard deviations from the mean. The Ramachandran plots were evaluated using PROCHECK, an application that analyzes the most allowed and banned areas of amino acid sequences, and the Z-score plots were studied by ProSA-web [64].

2.9. Disulfide Engineering of the Designed Vaccine

The stability of the designed model is required for docking analysis to begin. A protein structure with disulfide bonds is geometrically stable. For the intended vaccine, Disulfide by Design 2.0 [65] was utilized to assign such bonds.

2.10. Vaccine-TLR5 Docking

The binding linkages between modeling proteins and receptor molecules can be revealed by molecular docking. The refined vaccine model was submitted to the ClusPro v2.0 and HADDOCK server (version 2.4) as a ligand, and the PDB IDs of the MHC I (1I1Y), TLR5 (3V44), and MHC II (PDB ID: 1KG0) proteins were used as the immuno-logical receptors [29,66]. Using dynamic docking, HADDOCK designs biomolecular complexes based on existing information. The first stage was to separate the associated molecules from the protein structure in preparing the receptor; the second stage was the deletion of water and substances. The PyMOL v2.3.4 program was used for all of these processes [63]. To examine binding residues and interacting bonds on the surface, Discovery Studio 2017 and PBDSum were utilized.

2.11. MD Simulation

To determine whether TLR5 would bind strongly to the active site region of the designed vaccine, molecular dynamics simulations (MDS) of 111ns were applied [67]. The MDS was performed using the YASARA version 21.8.27.W.64 to analyze the thermodynamic stiffness of the vaccine-TLR5 complex [50,68]. YASARA is an intuitive and powerful tool for molecular dynamics simulations. Using AMBER14 force fields, it can predict parameters for macromolecules [50]. The physical mobility of atoms and molecules at the structural level, in addition to conformational alterations in clasped protein-ligand complexes, can be computed using molecular dynamics. As for MD simulations, the following parameters were kept: temperature 298 K, pressure at one bar, Coulomb electrostatics at a cutoff of 7.86, NaCl concentration 0.9%, pH 7, solvent density 0.997, time steps of one femtosecond (fs), periodic boundaries in one simulation box [69]. In the simulation cell, all analyses have been performed with the atoms sharing the same coordinates system. Finally, root mean square deviation (RMSD) and root mean square fluctuation (RMSF) computations were utilized to examine the conformational changes of docked complexes [70].

2.12. Simulation of Immune Response

C-IMMSIM v10.1, a server designed for assessing vaccine immunological responses, was used to analyze the construct [71]. The server verifies that in silico approaches may be used to improve vaccination dosages and immune responses in fish species [31]. Our minimum interval between doses was 30 days, as previously stated [72]. Within the in silico technique, three injections with time steps of 1, 84, and 168 were given, with one time step equaling 8 h in real life. All other stimulation parameters were kept at their usual levels, with the maximum simulation step value set at 300.

2.13. In Silico Cloning and Codon Adaptation

For foreign gene expression in a host, codon optimization is essential [73]. As a consequence, the construct was submitted to the JCat service (http://jcat.de/, accessed on 1 May 2022) for codon adaptation. This study utilized the commonly used *E. coli* K12 host, and all the processes were conducted while avoiding the following factors: sites of restriction enzyme cleavage, sites of binding of prokaryotic ribosomes, and rho-independent transcription termination. Evaluation of the modified sequence was done using the codon adaptation index (CAI) and guanine-cytosine (GC) concentration [73]. Finally, to clone the modified nucleotide sequence into the pET28a (+) expression vector, SnapGene v4.2 software was used to perform the in-silico cloning based on the modified nucleotide sequence [74].

3. Results

3.1. Analysis of Core Proteome

A majority of the target pathogen strains contain core proteins, meaning the inclusion of these proteins in vaccine formulations affords immune protection against a broader range of pathogens [75]. There have been 18 prominent pathogenic strains of *E. tarda* considered when designing vaccines against it. In total, these strains contained 332,753 proteins, but after core complete sequenced genomes analysis, this number was reduced to 12,539.

3.2. Identification of Proteins of Interest

Using several computational techniques and databases, subtractive proteomic analysis was used to examine the core complete sequenced genomes of *E. tarda*. A total of 12,539 proteins make up the core proteome. By excluding paralog sequences from 12,539 proteins, 477 proteins were retrieved via CD-HIT at an 80% threshold. Therefore, non-redundant proteins may not be directly targeted, since these proteins are not important for survival. Identification and discovery of essential proteins that are not similar to host proteins are critical for preventing drug cross-reactivity, since these proteins are required for pathogen survival [76]. A non-homologous essential protein was identified using BlastP. BlastP was used to identify 477 proteins with an identity of $\leq$30%, resulting in the identification of 297 essential proteins. A subcellular localization prediction model was used to obtain information about how specific proteins perform their functions. The studies excluded 163 targets predicted as cytoplasmic among the total 297 targets. As for the remaining 134 proteins (26 extracellular, 39 inner membranes, 41 outer membranes, and 28 periplasmic) (Supplementary Table S1), they were analyzed against the VFDB, resulting in 27 virulent proteins with a cutoff bit score greater than >100 and a sequence identity greater than $\leq$30%. VaxiJen v2.0 was used to evaluate the antigenicity of these proteins. The results confirmed 15 proteins to be highly antigenic among 27 proteins. Furthermore, eight proteins were shown to be lacking transmembrane helices. Additionally, six proteins were identified with molecular weights up to <110 kDa. All identified proteins showed as non-allergenic, thus making them excellent targets and candidates for vaccine development. The proteins in Table 1 are listed in detail.

Table 1. *E. tarda* vaccine candidate proteins are described in detail.

Name of Protein	Accession No.	Sub-Cellular Localization	Transmembrane Helices	Antigenicity	Molecular Weight (kDa)
MCP four-helix bundle domain-containing protein	WP_005281935.1	Inner Membrane	0	0.5040	55.87
Extracellular solute-binding protein	WP_035605308.1	Periplasmic	0	0.5105	37.86
Outer membrane protein A	ACY84110.1	Outer Membrane	0	0.6404	37.94
Hypothetical protein	WP_157757873.1	Extracellular	0	0.5833	35.22
Putative transporter protein	WP_005280555.1	Inner membrane	0	0.6064	58.95
Maltoporin protein	WP_005280774.1	Outer membrane	0	0.7530	47.10

3.3. Prediction of Epitopes

Our tests were performed on identified target proteins to find CTL and LBL epitopes. Both the CTLPred and Vaxitop servers predicted a total of 217 distinct T-cell epitopes with MHC-1 binding alleles. The top 11 non-toxic, non-allergenic, non-toxic, and immunogenic epitopes from the CTLPred server were compiled into a list. Additionally, the Vaxitop server projected antigenic, non-toxic, non-allergenic, and immunogenic properties for the top three T-cell epitopes (Table 2). Furthermore, 295 unique LBL epitopes were predicted, and nine of these were designed for MEBV based on their immunogenicity, antigenicity, and non-allergenicity (Table 3).

Table 2. Final T-cell epitopes.

Name of Server	Protein Name	Epitopes	Immunogenicity	Allergenicity	Antigenicity	Toxicity
CTLPred	MCP Four helix bundle domain-containing protein	QTNILALNA	Positive	Negative	0.6679	Negative
	MCP Four helix bundle domain-containing protein	LMLILAGLA	Positive	Negative	0.4431	Negative
	Extracellular solute-binding protein	LSMRARVLY	Positive	Negative	0.6913	Negative
	Extracellular solute-binding protein	AASLLFGLS	Positive	Negative	0.4425	Negative
	Outer membrane protein A	YTDRIGSDQ	Positive	Negative	1.0949	Negative
	Outer membrane protein A	PLAAIGVEY	Positive	Negative	0.7107	Negative
	Hypothetical protein	MSLVLKIIP	Positive	Negative	1.2527	Negative
	Putative transporter protein	LLALLFWSV	Positive	Negative	2.0790	Negative
	Putative transporter protein	PQLLALLFW	Positive	Negative	2.1342	Negative
	Maltoporin protein	MIDFYYWDI	Positive	Negative	2.5781	Negative
	Maltoporin protein	GSLELGFDY	Positive	Negative	1.2685	Negative
Vaxitop Server	Extracellular solute-binding protein	INTWLRLGAASLLFG	Positive	Negative	1.0671	Negative
	Outer membrane protein A	GAFFGYQANPYLGFE	Positive	Negative	2.2112	Negative
	Maltoporin protein	MTASNSGHSGGSSVN	Positive	Negative	2.0832	Negative

Table 3. Final LBL epitopes.

Protein Name	Sequence	Position	Score	Antigenicity	Allergenicity
MCP four-helix bundle domain-containing protein	FLMLILAGLAAA	200	0.52	0.8265	Negative
MCP four-helix bundle domain-containing protein	GLTSGSGELAAR	291	0.55	1.5861	Negative
Outer membrane protein A	PAPIPAPAPAPV	203	0.74	0.9919	Negative
Outer membrane protein A	YQYVNKVGTRSE	166	0.57	1.0305	Negative
Hypothetical protein	SVSAVDIEKRQA	221	0.53	0.9263	Negative
Putative transporter	ARLVIGEQVDTS	270	0.75	0.7535	Negative
Putative transporter	SRNGHHHELLQT	195	0.71	1.0494	Negative
Maltoporin	TNPGGSLELGFD	206	0.74	1.3095	Negative
Maltoporin	GAGSKYRLGNEC	51	0.73	1.9150	Negative

3.4. Epitope and Allele Docking Studies

To confirm that selected epitopes are capable of binding HLA alleles, docking was employed. There are also docking alleles, binding affinities, interactions, and residues that form hydrogen bonds with epitopes, summarized in Table 4. 15-mer epitopes had affinity ranges from −6.7 to −9.1 kcal/mol (Table 4). Notwithstanding the tabulated details, we introduced the top two best associating MTASNSGHSGGSSVN and GAFFGYQANPYLGFE epitopes in the HLA-DAB1*15:01 and HLA-B*3501 allele, respectively. The best epitope

generated 16 hydrogen bonds in total, 14 of which were classical interactions with the active site residues Tyr7, Arg2, Asp9, Glu63, Lys66, Arg69, Asn77, Asn77, Lys80, Tyr84, Tyr99, Thr143, Lys146, Trp147, Glu15, and Glu152.

Table 4. List of docking alleles, binding affinities, interactions, and residues that form hydrogen bonds with epitopes.

T-Cell Epitope	HLA Allele	Epitope Affinity (kcal/mol)	Control Affinity (kcal/mol)	Number of Hydrogens Bonds (CHB)	Residues Involved in CHB Networks (n)
INTWLRLGAASLLFG	DAB1*07:01	−7.2	−6.9	9 (7)	Met69, Ala149, Thr7, Ile8, Gln19, Ile1, Ala2, Trp7, Tyr74 (9)
GAFFGYQANPYLGFE	DAB1*15:01	−7.2	−7.1	8 (7)	Tyr80, Lys84, Val146, Thr7, Lys9, Val66, Thr77, Asn143 (8)
MTASNSGHSGGSSVN	DAA2*01:01	−7.1	−7.0	16 (14)	Tyr7, Asp2, Asp9, Glu63, Lys66, Arg69, Asn77, Asn77, Lys80, Tyr84, Tyr99, Thr143, Lys146, Trp147, Glu15, Glu152 (16)
INTWLRLGAASLLFG	HLA-A*0201	−6.7	−7.3	9 (7)	Arg71, Ala12, Asn82, Val1, Glu6, Ser4, Thr77, Thr13, Val14 (9)
GAFFGYQANPYLGFE	HLA-B*3501	−7.1	−7.9	12 (10)	Tyr7, Asp9, Asp9, Ser24, Glu63, Lys66, Arg69, Arg69, Tyr99, Glu152, Glu152, Gln155 (12)
MTASNSGHSGGSSVN	HLA-B*3508	−6.9	−7.3	9 (8)	Ser63, Glu85, Asn72, Trp326, His7, Glu45, Phe17, Phe8, Ile17 (9)

3.5. Construction of Final Vaccine

The vaccine was constructed with 23 epitopes from two different classes that had already been chosen. AAY, GPGPG, and KK linkers were used to connect epitopes. An adjuvant was used before the construct to improve immunogenicity. The EAAAK linker was used to bind an adjuvant to the CTL epitope to activate TLR5 using the ribosomal protein the 50S/L12 as an agonist. The final immunization was 450 amino acids in length (Figure 2).

MAKLSTDELLDAFKEMTLLELSDFVKKFEETFEVTAAAPVAVAAAGAAPAGAAVEAAEEQSEFDVILEAAGDKKIG
VIKVVREIVSGLGLKEAKDLVDGAPKPLLEKVAKEAADEAKAKLEAAGATVTVKEAAAKQTNILALNAAAYLMLILA
GLAAAYLSMRARVLYAAYAASLLFGLSAAYYTDRIGSDQAAYPLAAIGVEYAAYMSLVLKIIPAAYLLALLFWSVAAY
PQLLALLFWAAYMIDFYYWDIAAYGSLELGFDYGPGPGINTWLRLGAASLLFGGPGPGGAFFGYQANPYLGFEGP
GPGMTASNSGHSGGSSVNKKFLMLILAGLAAAKKGLTSGSGELAARKKPAPIPAPAPAPVKKYQYVNKVGTRSEK
KSVSAVDIEKRQAKKARLVIGEQVDTSKKSRNGHHHELLQTKKTNPGGSLELGFDKKGAGSKYRLGNEC

Figure 2. Constructed vaccine sequence.

3.6. Immunological Assessment and Physicochemical Characteristics

The molecular weight of the construct was determined to be 47,284.67 Da. Other characteristics included the theoretical isoelectric point (pI) of 8.82, chemical formula $C_{2157}H_{3410}N_{552}O_{620}S_9$, instability index of 28.48, aliphatic index of 96.29, and grand average of hydropathicity of 0.122. The physicochemical characteristics and immunological effects of the construct were also evaluated. The construct, for example, has an antigenicity of 0.7818 and immunogenicity of 1.47082. With a score of 0.891343 out of 1, the vaccine was also confirmed to be soluble (Table 5). As secondary structural properties, alpha-helix, beta-strand, and random coils were investigated using two different servers. In the build, it predicted α-helices at 41.79%, β-strands at 25.75%, and random coils at 23.13%. The

PSIPRED server, on the other hand, predicted 43.84% α-helix, 20.71% β-strand, and 35.47% random coils (Figure 3).

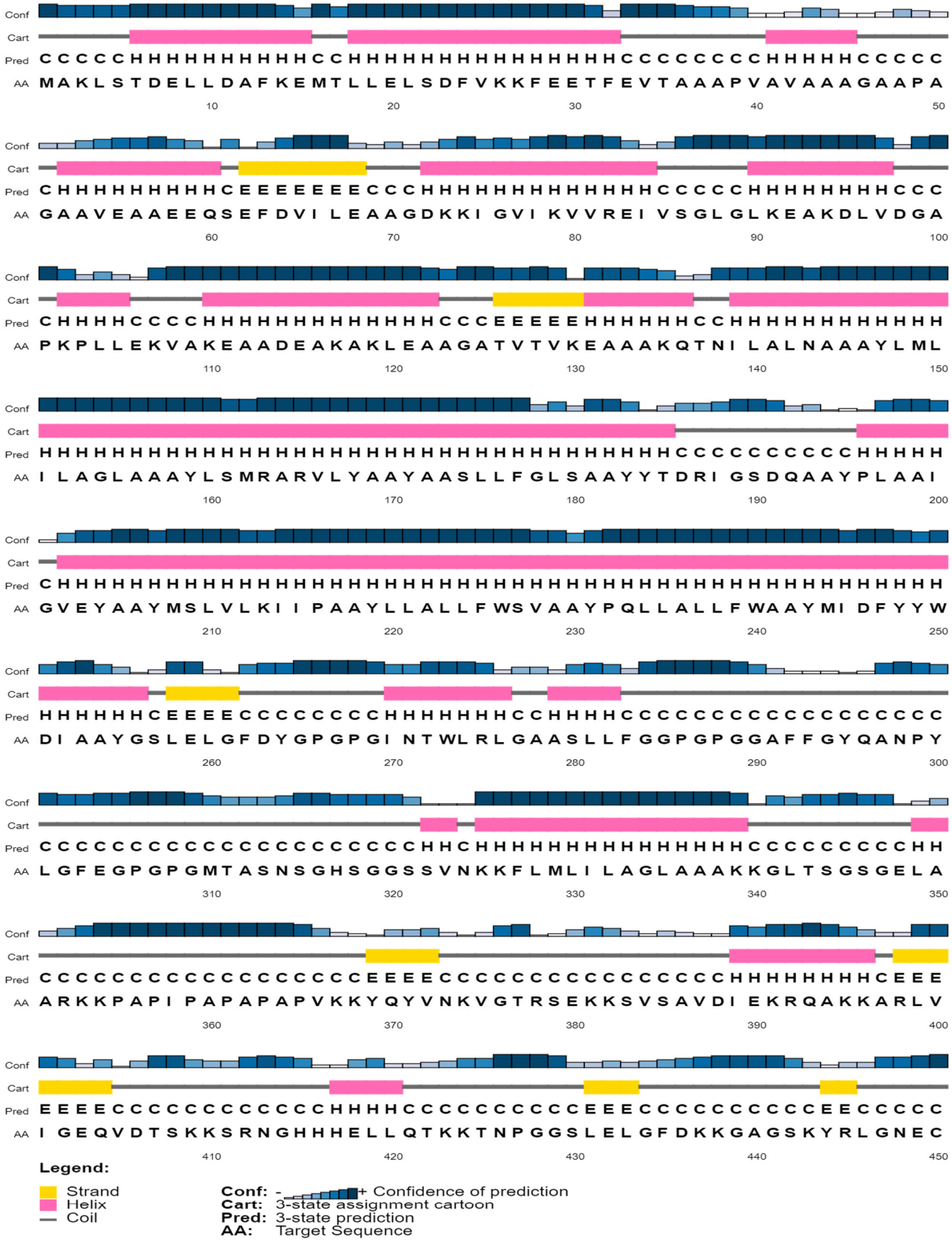

Figure 3. Prediction of the secondary structure of designed multi-epitope vaccines using PSI-PRED.

Table 5. Antigenicity, allergy, and physicochemical features of the construct.

Characteristics	Finding	Remark
Number of amino acids	450	Suitable
Molecular weight	47,284.67	Average
Theoretical pI	8.82	Base
Chemical formula	$C_{2157}H_{3410}N_{552}O_{620}S_9$	-
Instability index of vaccine	28.48	Stable
Aliphatic index of vaccine	96.29	Thermostable
Grand average of hydropathicity (GRAVY)	0.122	Hydrophobic
Antigenicity	0.7818	Antigenic
Immunogenicity	1.47082	Immunogenic
Allergenicity	No	Non-allergen
Solubility	0.891343	Soluble

3.7. 3D Structure Refinement and Confirmation

RaptorX was used as the best template to create the top five homology models. We chose the model with the lowest C-score (−4.97) out of the five. Figure 4 shows a 3D illustration of the finished vaccination. After refining, the vaccine (model 1) had 80.9% residues in the Ramachandran plot's most preferred area. The modified 3D vaccine model was further evaluated using the ProSA-web servers. The vaccine's Ramachandran plot indicated 80.7% of residues in the most favorable zone, 15.7% in the additional acceptable region, and 1.6% in the prohibited region before refining. Nevertheless, following refinement, the Ramachandran plot revealed 80.9% of the residues in the most favorable zone, 14.9% in additional authorized regions, and 0.8% in prohibited regions (Figure 5B). The Z score was −5.09 for the crude models, whereas the Z-score was −6.11 for the refined model (Figure 5D).

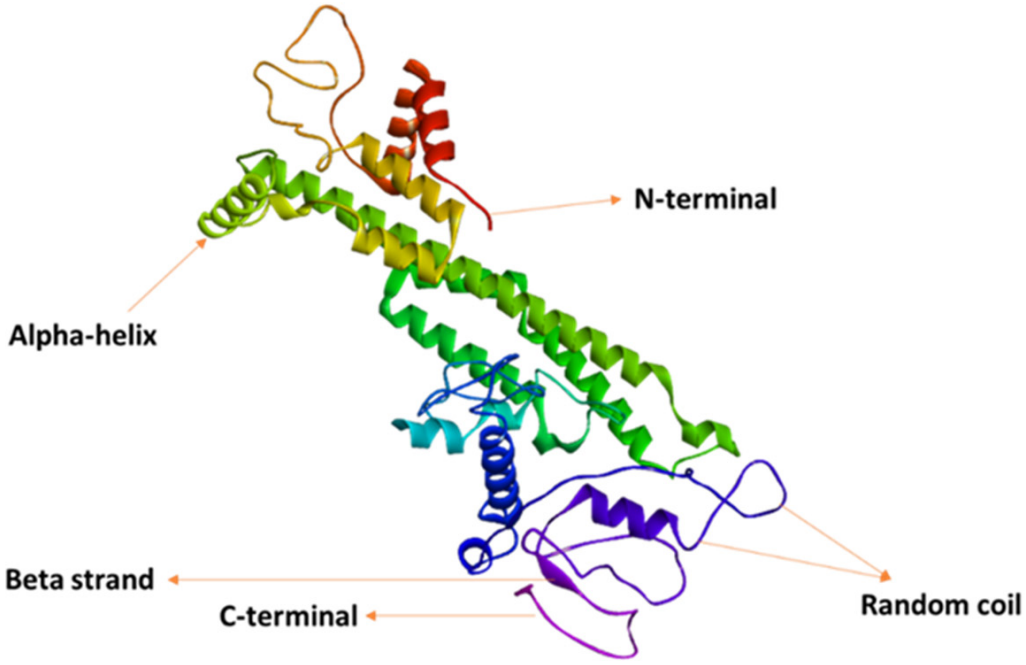

Figure 4. The designed vaccine construct's 3D structure.

3.8. Vaccine Disulfide Engineering

The vaccine design was stabilized through disulfide engineering. In our vaccine, the DbD2 server detected 30 pairings of amino acids that have the potential to generate disulfide bonds. Two cysteine mutation pairs were recommended, along with energy and chi3. Thus,

the residue pairs with the most mutations were SER27-CYS51 and LEU74-CYS95. Energy and chi3 have been approved with values less than 4.83 and 100.39: −111.54, respectively.

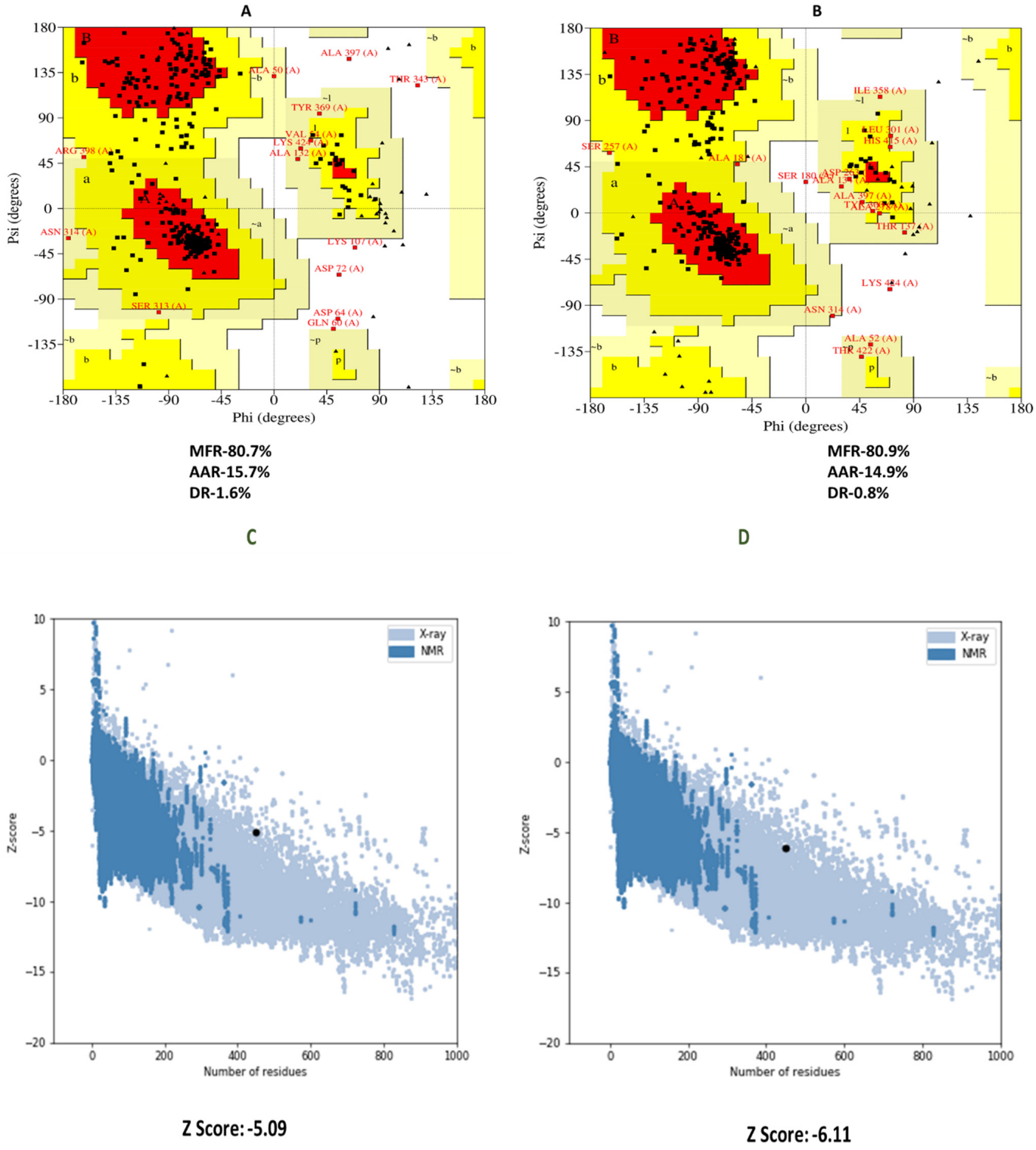

Figure 5. PROCHECK server Ramachandran plot analysis (**A**,**B**). The most preferred, additional allowed, generously allowed, and forbidden areas of the vaccination were symbolized as the MFR, AAR, GAR, and DR. (**C**,**D**) Pro-SA server validates the 3D structure with a Z-score.

3.9. Molecular Docking Research

To predict binding affinity and interactions, docking analysis was performed between the vaccine sequence as ligand and TLR5, MHC I, and MHC II as receptors. This method resulted in the appearance of ten docked complexes of varying sizes on the ClusPro v2.0 server. Among the complexes, the binding posture with functional contacts and the complex with the lowest energy score were chosen. After docking ligan and receptors, we chose model 1 for each complex based on their energy score. The energy score of the three complexes, Vaccine-TLR5, Vaccine-MHC I, and Vaccine-MHC II, was −956.5, −921.5, and −890.5, respectively. We also predicted the docking statistics of these three complexes through the HADDOCK server (Table 6). The PDBsum server examined interactions between vaccines and residues found in the active site residues of selected complexes. The interaction surface of the Vaccine-TLR5 receptor complex contains a total of 17 hydrogen bonds. Among them, there were 13 classical hydrogen bonds. The interacting residues of the vaccine were Asp 100, Asp99, Arg 106, Thr 116, Thr 115, Ser 103, Asp 101, Arg 96, Glu 111, Gly 110, Thr 112, Lys 109, and Ala217 (Figure 6A). In addition, in Vaccine-MHC I complexes, a total of 17 hydrogen bonds were found; among them, 11 were classical. The interacting residues are Arg 12, Asp 98, Asn 24, Tyr 10, Met 99, Gln 8, Ser 28, His 31, Arg 3, Trp 60, and Asp 53 (Figure 6B). However, we found only two hydrogen bonds in Vaccine-MHC II such as Tyr 171 and Tyr 219. Furthermore, Figure 6C shows residues associated with TLR5, MHC I, and MHC II active sites.

Table 6. Vaccine docking with immune receptors and MHC molecules.

Features	MEBV-MHCI	MEBV-MHCII	MHC-TLR5
HADDOCK Score	211.3 ± 12.2	169.4 ± 22.3	207.6 ± 14.6
Cluster Size	6	5	7
Van der Waals energy	−41.8 ± 3.6	−69.1 ± 2.2	−41.1 ± 2.3
Desolvation energy	−1.4 ± 0.7	−12.7 ± 4.8	−0.5 ± 3.3
Electrostatic energy	−60.8 ± 9.0	−261.1 ± 24.8	−67.1 ± 27.8
RMSD from the overall lowest-energy structure	37.6 ± 0.3	9.3 ± 0.5	49.4 ± 0.1
Buried surface area	2219.9 ± 110.2	2977.6 ± 63.1	2101.9 ± 120.9
Z-Score	−1.1	−0.9	−1.9
Restraint violation energy	2746.2 ± 114.9	3124.6 ± 172.4	2529.9 ± 182.4

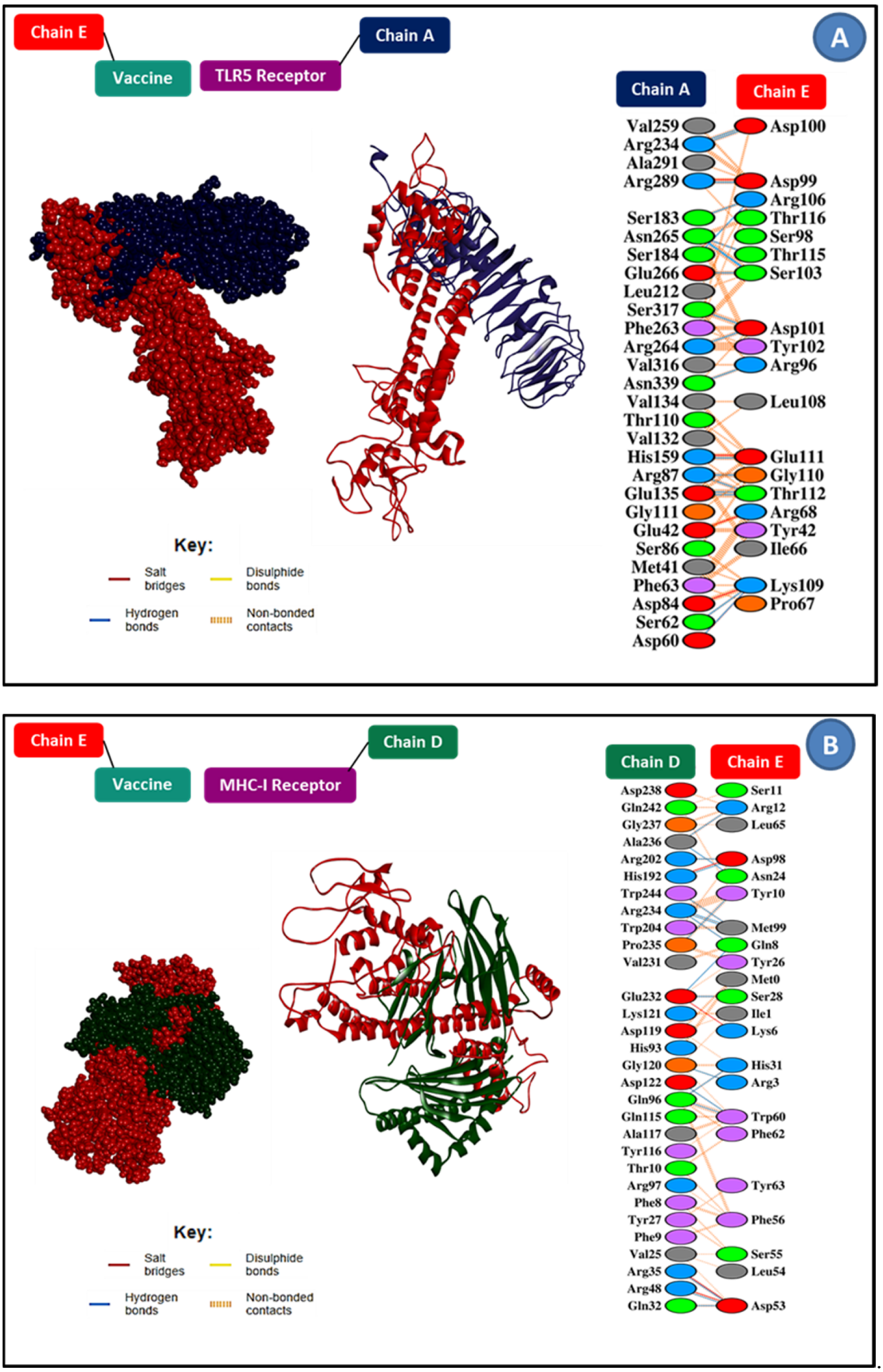

Figure 6. Cont.

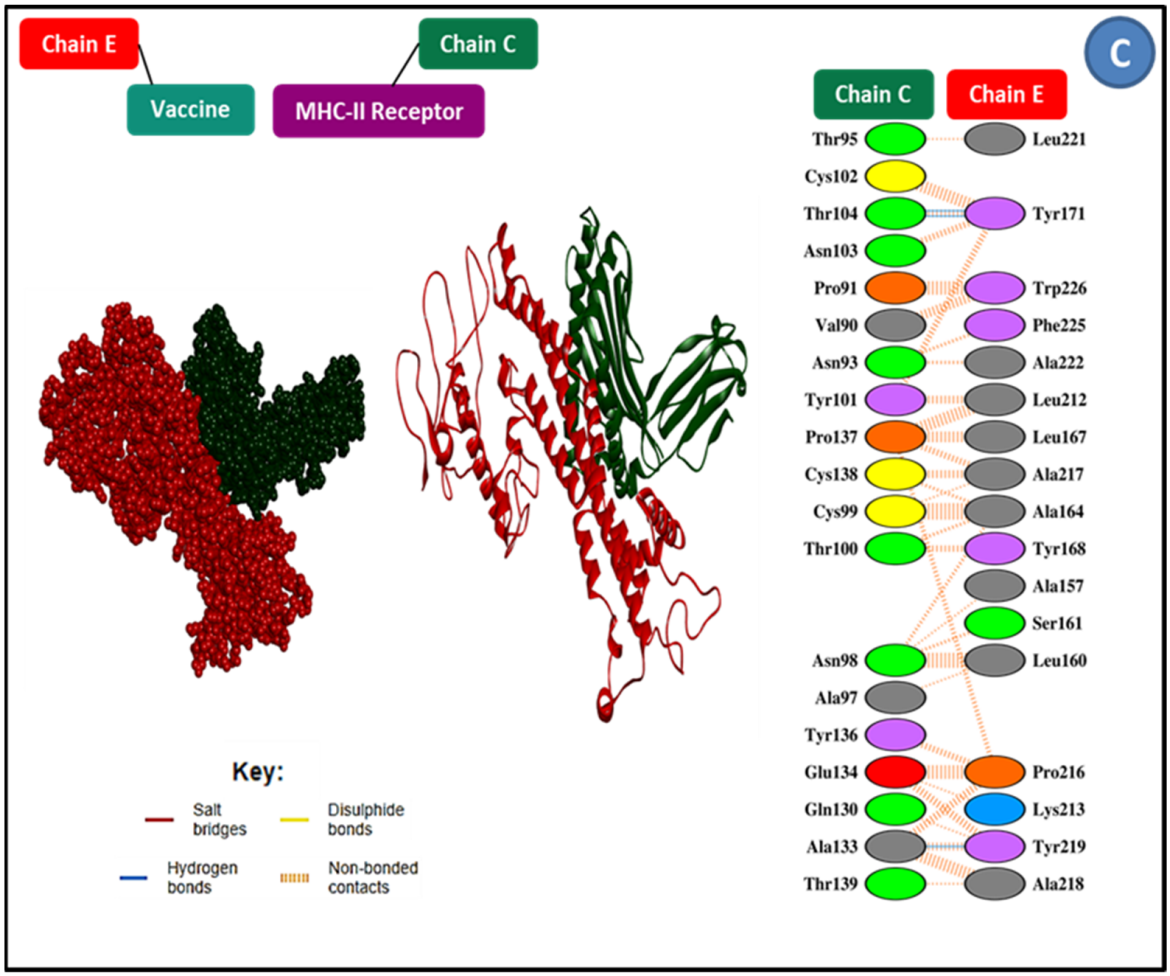

Figure 6. Analysis of EBV—immune receptor binding conformation and interaction (**A**) MEBV-TLR5, (**B**) MEBV-MHC I, and (**C**) MEBV-MHC II.

3.10. MD Simulation

To determine whether TLR5 would bind strongly to the active site region of the designed vaccine, molecular dynamics simulations (MDS) of 111ns were applied [67]. The MDS was performed using the YASARA version 21.8.27.W.64 to analyze the thermodynamic stiffness of the vaccine-TLR5 complex [50,68]. YASARA is an intuitive and powerful tool for molecular dynamics simulations. Using AMBER14 force fields, it can predict parameters for macromolecules [50]. Molecular dynamics may be used to calculate the functional ability of molecules at the structural level, as well as the conformational changes that take place in protein-ligand docked complexes. As for MD simulations, the following parameters were kept: temperature 298 K, pressure at one bar, Coulomb electrostatics at a cutoff of 7.86, NaCl concentration 0.9%, pH 7, solvent density 0.997, time steps of one femtosecond (fs), and periodic boundaries in one simulation box [69]. In the simulation cell, all analyses have been performed with the atoms sharing the same coordinates system. Lastly, to analyze the conformational changes of docked complexes, root mean square deviation (RMSD) (Figure 7) and root mean square fluctuation (RMSF) (Figure 8) calculations were used [70].

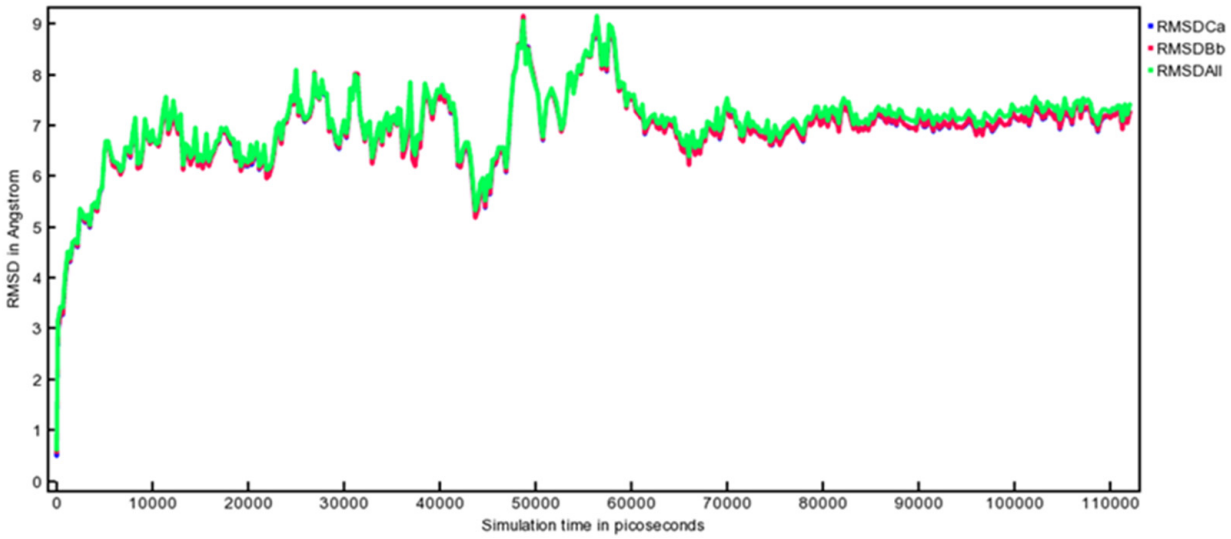

Figure 7. Simulation of the final vaccine sequence using molecular dynamics. The RMSD technique was used to visualize the backbone atoms of the complexes.

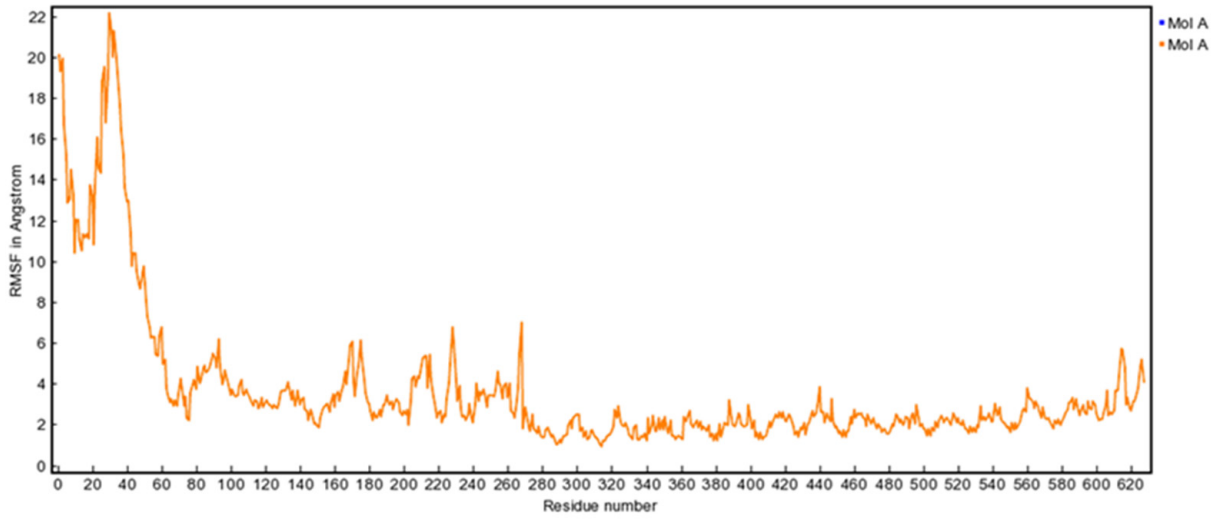

Figure 8. Molecular dynamic simulation analysis of the vaccine. The multi-epitope docked vaccine candidate RMSF plot.

3.11. Immune Response Simulation

Computer-based immune responses approximated true immunological responses triggered by some diseases (Figure 9). For example, secondary and tertiary immune responses were larger than the initial responses (Figure 9A). Secondary and tertiary reactions were also seen, which were related to improved antibody levels and resulted in considerably better antigen clearance following successive exposures (Figure 9A). B-cells, cytotoxic T-cells, and helper T-cells also showed a prolonged survival duration, indicating IgM memory formation and immune cell class switching (Figure 9B–D). Th0 type immune reactions were less frequent (%) and more numerous (cells/mm^3) than Th1 type immune reactions (Figure 9I). During the presentation, increased macro-phage mobility was seen, whereas dendritic cell movement was expected (Figure 9F,G).

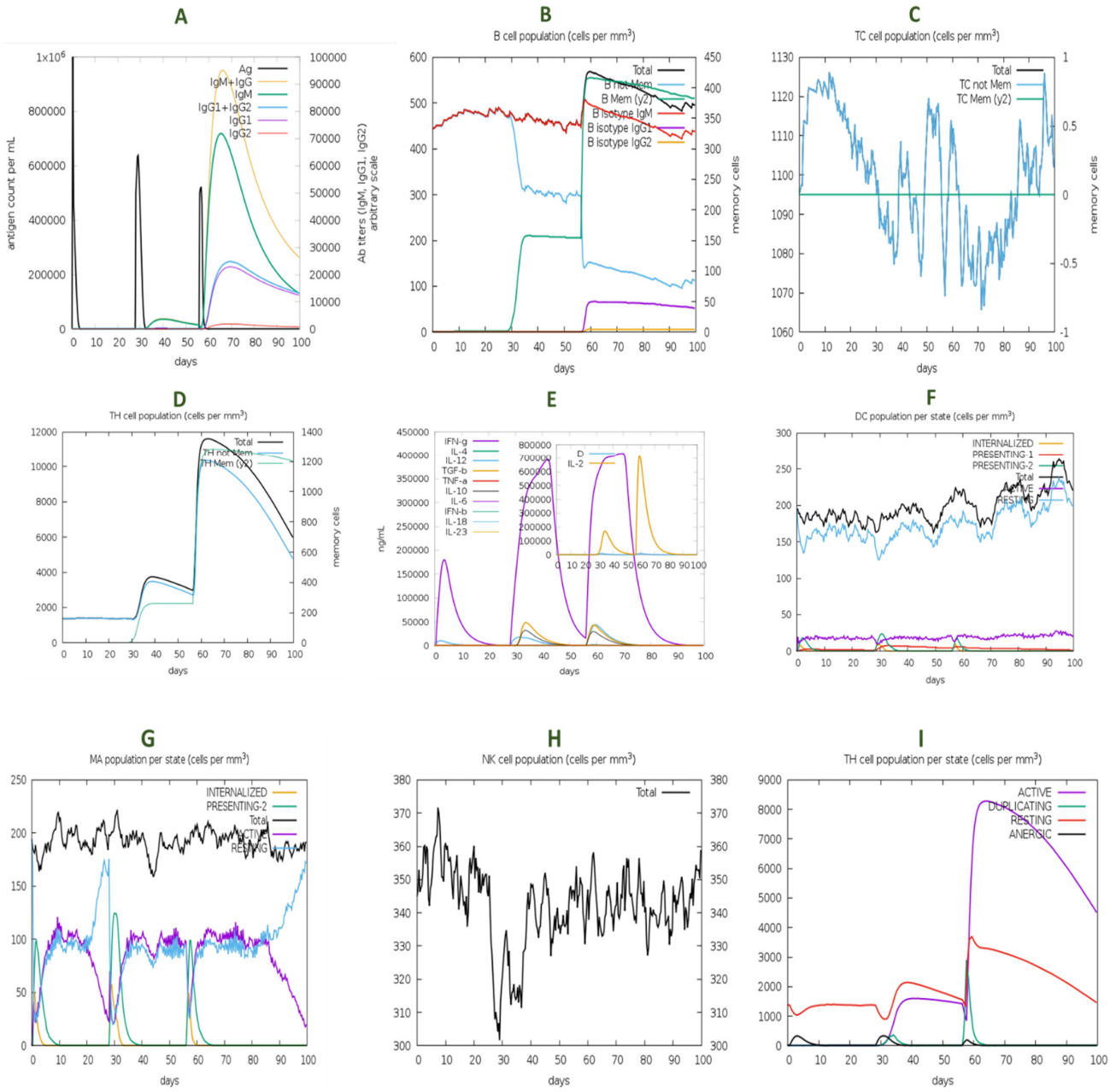

Figure 9. An immunological response has been generated by the vaccine. The graph depicts (**A**) vaccine immune responses, (**B**) B-cell population, (**C**) cytotoxic T-cell population, (**D**) helper T-cell population, (**E**) cytokine and interleukin induction, (**F**) dendritic cell population per state, (**G**) macrophage population per state, (**H**) Natural Killer cells (total count), and (**I**) percentage (percent) and amount (cells/mm^3) of Th1-mediated immunity.

3.12. In Silico Cloning and Codon Adaptation

In this study, the codons according to the *E. coli* K12 on the JCat service were changed to optimize the vaccine design's translation efficiency. The peptide vaccine constructs generated a total of 804 nucleotide sequences (450 AA residues) (Figure 10). The reverse nucleotide sequence had a GC content of 55.78% and a CAI value of 1.0, according to further studies. The restriction sites XhoI and BamHI were used as the start and end cut points, respectively, to insert the altered sequence into the pET28a (+) vector. SnapGene was used to clone the modified vaccine design into the cloning vector pET28a (+) (Figure 11).

```
ATGGCGAAACTGAGCACCGATGAACTGCTGGATGCGTTTAAAGAAATGAC      50
CCTGCTGGAACTGAGCGATTTTGTGAAAAAATTTGAAGAAACCTTTGAAG     100
TGACCGCGGCGGCGCCGGTGGCGGTGGCGGCGGCGGGCGCGGCGCCGGCG     150
GGCGCGGCGGTGGAAGCGGCGGAAGAACAGAGCGAATTTGATGTGATTCT     200
GGAAGCGGCGGGCGATAAAAAAATTGGCGTGATTAAAGTGGTGCGCGAAA     250
TTGTGAGCGGCCTGGGCCTGAAAGAAGCGAAAGATCTGGTGGATGGCGCG     300
CCGAAACCGCTGCTGGAAAAAGTGGCGAAAGAAGCGGCGGATGAAGCGAA     350
AGCGAAACTGGAAGCGGCGGGCGCGACCGTGACCGTGAAAGAAGCGGCGG     400
CGAAACAGACCAACATTCTGGCGCTGAACGCGGCGGCGTATCTGATGCTG     450
ATTCTGGCGGGCCTGGCGGCGGCGTATCTGAGCATGCGCGCGCGCGTGCT     500
GTATGCGGCGTATGCGGCGAGCCTGCTGTTTGGCCTGAGCGCGGCGTATT     550
ATACCGATCGCATTGGCAGCGATCAGGCGGCGTATCCGCTGGCGGCGATT     600
GGCGTGGAATATGCGGCGTATATGAGCCTGGTGCTGAAAATTATTCCGGC     650
GGCGTATCTGCTGGCGCTGCTGTTTTGGAGCGTGGCGGCGTATCCGCAGC     700
TGCTGGCGCTGCTGTTTTGGGCGGCGTATATGATTGATTTTTATTATTGG     750
GATATTGCGGCGTATGGCAGCCTGGAACTGGGCTTTGATTATGGCCCGGG     800
CCCGGGCATTAACACCTGGCTGCGCCTGGGCGCGGCGAGCCTGCTGTTTG     850
GCGGCCCGGGCCCGGGCGGCGCGTTTTTTGGCTATCAGGCGAACCCGTAT     900
CTGGGCTTTGAAGGCCCGGGCCCGGGCATGACCGCGAGCAACAGCGGCCA     950
TAGCGGCGGCAGCAGCGTGAACAAAAAATTTCTGATGCTGATTCTGGCGG    1000
GCCTGGCGGCGGCGAAAAAAGGCCTGACCAGCGGCAGCGGCGAACTGGCG    1050
GCGCGCAAAAAACCGGCGCCGATTCCGGCGCCGGCGCCGGCGCCGGTGAA    1100
AAAATATCAGTATGTGAACAAAGTGGGCACCCGCAGCGAAAAAAAAAGCG    1150
TGAGCGCGGTGGATATTGAAAAACGCCAGGCGAAAAAAGCGCGCCTGGTG    1200
ATTGGCGAACAGGTGGATACCAGCAAAAAAAGCCGCAACGGCCATCATCA    1250
TGAACTGCTGCAGACCAAAAAAACCAACCCGGGCGGCAGCCTGGAACTGG    1300
GCTTTGATAAAAAAGGCGCGGGCAGCAAATATCGCCTGGGCAACGAATGC
```

Figure 10. Codon adaptation of EBV to *E. coli* K12 strain.

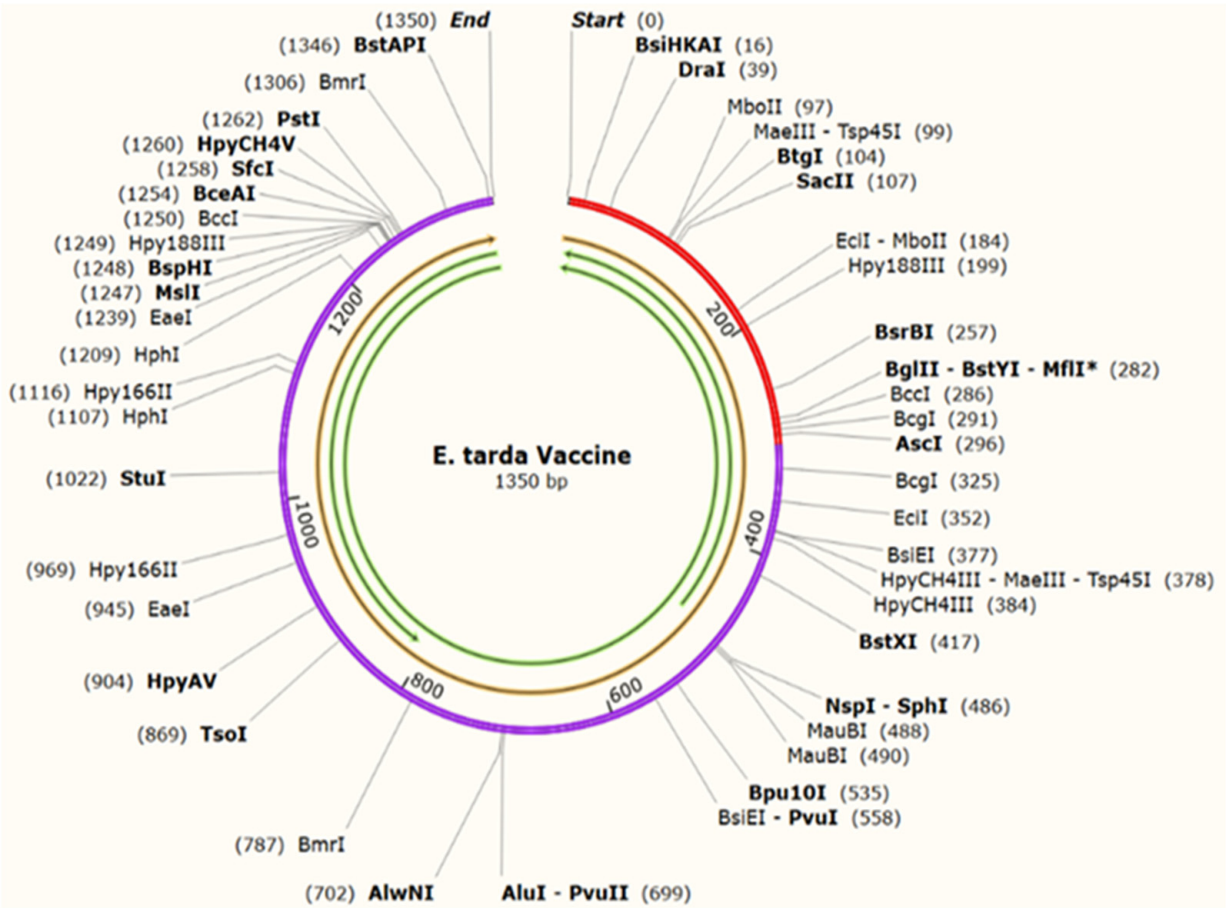

Figure 11. In silico cloning of the proposed vaccine into the pET-28a (+) vector.

4. Discussion

Edwardsiella tarda (*E. tarda*) infects both aquatic and terrestrial fishes, reptiles, amphibians, and mammals throughout the world. Unlike other *Edwardsiella* species, *E. tarda* is zoonotic and can infect humans. In some cases, it can cause long-term chronic infection in humans. Thus, therapeutic control of the infection from this antibiotic-resistant pathogen is pivotal. Previously, in Osteichthyes species, a gene lineage of MHC class II molecules and three MHC class I molecules have been found [22]. Bony fishes are among the most diverse group of vertebrates within the class Osteichthyes, which includes both marine and freshwater species of fish. The researchers found that the sub-lineage E genes of MHC II molecules, which are non-polymorphic and have a poor expression in the tissues of the immune system, can be found in primitive fishes, i.e., in paddlefish, sturgeons, and spotted gar, as well as in cyprinids, Atlantic salmon, Euro-pean seabass, channel catfish, turbot, and rainbow trout [22]. In fish, three MHC II molecule sublineages (MHC II-A, -B, and -E) have been found. Among others, zebrafish, Atlantic salmon, medaka, Nile tilapia, three-spine sticklebacks, spotted green pufferfish, and Mexican tetra possess MHC I-U and -Z lineage molecules [22]. In contrast, all of the MHC I and MHC II molecule lines, each with a distinct number of genes, were only discovered in Atlantic salmon [20].

Current outbreaks of *E. tarda* pose a threat to the global aquaculture industry, so the aim of this study was to design a vaccine using an immunoinformatics and in silico approach. At first, the study aimed to select the most virulent and antigenic protein by applying the core complete sequenced genomes analysis of *E. tarda* genome from the NCBI database. Based on the virulent protein, the vaccine exhibited excellent relevance and subsequently proved to be reliable, as predicted by immunoinformatics. As prophylaxis, vaccines protect against infection and illnesses safely and effectively [77]. With the right immunizations, protection against infectious diseases can be built [78]. In the absence of an effective vaccine, *E. tarda* infection and transmission are difficult to prevent and manage. Moreover, an effective vaccine has yet to be developed to control the current condition. As a result, identifying a response to the economically threatening problems will need a unique vaccine development technique. We set out to design an epitope vaccine focusing on the most virulent protein of *E. tarda* since the OMP (outer membrane protein) and other virulent proteins are essential for immunological invasion and transmission within fish species. To allow cellular and humoral immune systems to detect this protein, the antigenic region of every pathogenic protein chosen by in silico screening was assessed. Identifying all probable T-cell and B-cell epitopes was the initial step. Since the linkers are related to the top epitopes, vaccines were developed with 23 antigenic epitopes. Both MHC class I and class II molecules were found in the Atlantic cord and tilapia [22]; therefore, we detailed the interactions between this allele with the selected 15-mer epitopes and the result was acceptable. T-cell and B-cell epitopes were employed in vaccine development as a key component for improving the peptide vaccine's stability, folding, and transcriptional regulation [55,79]. EAAAK linkers bind adjuvants to T-cell epitopes, making the vaccine more stable and persistent while also improving cellular and humoral immunogenic responses [55,80]. The vaccine was discovered to have 450 amino acid residues in total. Solubility, a form of physicochemical property, is an important feature of a recombinant vaccine [81]. The vaccine design was tested for solvability inside the host *E. coli* using a solubility evaluation tool, and the findings revealed that it was. The developed vaccine had an acidic character, as shown by the predicted PI value. The vaccine sequence's stability index, as determined using server tools, demonstrates that it will be stable following synthesis. The GRAVY value and aliphatic index, on the other hand, indicated that the vaccine was hydrophilic and thermostable. According to the predicted physicochemical qualities and overall scores, this vaccine has a good chance of becoming a viable option against *E. tarda*. After the 3D structure prediction, the identified models were reviewed, and the best model was selected (based on the c-score). The Z-score (–6.11) and most productive components of the most favored, acceptable, and prohibited areas for the Ramachandran plot were noted during the validation check of the 3D structure. This was indicated by the lowest energy scores

of −956.5, −921.5, and −890.5 obtained from a molecular docking of the vaccine-TLR5, vaccine-MHC I, and vaccine-MHC II complexes, respectively; the vaccination might have an infection-inhibiting function and engage firmly with these receptors. In a molecular docking study between the peptide vaccine and TLR5 receptor, the vaccine binding the convenient TLR5 receptor was found to have the lowest energy score of −956.5, suggesting the vaccine would reduce infection. The molecular dynamics simulation has the potential to help researchers quickly identify how proteins work and how their structure is formed. Dynamic simulation of the protein-receptor complex as a function of time can be used to generate anatomical movement. RMSD and RMSF scores were used to examine the results of 111 ns dynamic simulations of the vaccine candidate. When comparing one atomic conformation to another in a molecular system, RMSD is used. As the atoms of a certain vaccine candidate depart from the receptor structure, the result determines its significant plasticity using the RMSD value of the receptor structure, as well as its movement based on the RMSF of its complex configuration. The designed average RMSD and RMSF values were 6.32 Å and 4.0 Å, respectively. In the vaccine segment, the variance was not as high; however, after 70 nano-seconds, it smoothed out, showing that the modeled vaccination and receptor are stable. An immunological simulation of target clearance and cell density was used to evaluate the optimum immunologic response to the pathogen. The immune system produced memory B-cells as a result of the increased vaccine dosages. In this way, the vaccination successfuly replicated a humoral immune response to increased immunoglobulin synthesis. MD simulations were used to determine the rigidity of the vaccine with the receptor, and codon optimization was used to improve epitope vaccine synthesis inside the host. In silico cloning of the expected immunization up-and-comer into the *E. coli* K12 expression have pET28a (+) vector was effective when the codon was adjusted. In addition, this designed vaccine sequence is not based on the evidence produced or experimented with in vivo. Therefore, wet lab analysis is needed to support the use of the immunoinformatic approach for successful vaccination.

5. Conclusions

This study employed a variety of computational algorithms to identify potential B and T-cell epitopes in *E. tarda* pathogenic proteins, which were then stitched together into a multi-epitope vaccine. The immuno-dominant properties desired in a vaccine have just been discovered. It might potentially bind to immunological receptors and trigger a powerful immune response against *E. tarda* disease. In light of our discoveries, we recommend that making an immunization against the etiological go-between of the *E. tarda* scourge in fish ought to start with the immunization applicant. In addition, the possible epitopes discovered in this study can be employed in future studies. However, further research is needed to prove that our vaccine is an effective *E. tarda* preventive.

Supplementary Materials: The following supporting information can be downloaded at: https://www.mdpi.com/article/10.3390/applmicrobiol2020031/s1, Table S1: List of subcellular localization of 134 proteins of *E. tarda*.

Author Contributions: Conceptualization, S.I.I., S.S. and M.J.I.; methodology, S.I.I.; software, S.I.I. and S.M.; validation, S.I.I., M.J.M. and M.J.I.; formal analysis, S.I.I. and S.M.; investigation, S.I.I.; resources, S.I.I.; data curation, S.I.I.; writing—original draft preparation, S.I.I. and M.J.I.; writing—review and editing, S.I.I. and M.J.I.; visualization, S.I.I.; supervision, S.M. All authors have read and agreed to the published version of the manuscript.

Funding: This research received no external funding.

Institutional Review Board Statement: Not applicable.

Informed Consent Statement: Not applicable.

Data Availability Statement: Not applicable.

Acknowledgments: The authors of this manuscript are very much thankful to the BiosoL center for its technical support.

Conflicts of Interest: The authors declare no conflict of interest.

References

1. Hassan, H.A.; Ding, X.; Zhang, X.; Zhu, G. Fish borne *Edwardsiella tarda* eha involved in the bacterial biofilm formation, hemolytic activity, adhesion capability, and pathogenicity. *Arch. Microbiol.* **2020**, *202*, 835–842. [CrossRef] [PubMed]
2. Mohanty, B.R.; Sahoo, P.K. Edwardsiellosis in fish: A brief review. *J. Biosci.* **2007**, *32*, 1331–1344. [CrossRef] [PubMed]
3. Evans, J.J.; Klesius, P.H.; Plumb, J.; Shoemaker, C.A. *Edwardsiella Septicaemias*; CABI: Wallingford, UK, 2011; pp. 512–569.
4. Lima, L.C.; Fernandes, A.A.; Costa, A.A.P.; Velasco, F.O.; Leite, R.C.; Hackett, J.L. Isolation and characterizaton of Edwardsiella tarda from pacu Myleus micans. *Arqic. Bras. Med. Vet. Zootec.* **2008**, *60*, 275–277. [CrossRef]
5. Van Damme, L.R.; Vandepitte, J. Frequent isolation of Edwardsiella tarda and Pleisiomonas shigelloides from healthy Zairese freshwater fish: A possible source of sporadic diarrhea in the tropics. *Appl. Environ. Microbiol.* **1980**, *39*, 475–479. [CrossRef] [PubMed]
6. Sun, K.; Wang, H.-L.; Zhang, M.; Xiao, Z.-Z.; Sun, L. Genetic Mechanisms of Multi-Antimicrobial Resistance in a Pathogenic *Edwardsiella tarda* Strain. *Aquaculture* **2009**, *289*, 134–139. [CrossRef]
7. Wang, Y.; Zhang, X.H.; Austin, B. Comparative analysis of the phenotypic characteristics of high-and low virulent strains of Edwardsiella tarda. *J. Fish Dis.* **2010**, *33*, 985–994. [CrossRef]
8. Zhang, M.; Sun, K.; Sun, L. Regulation of autoinducer 2 production and luxS expression in a pathogenic Edwardsiella tarda strain. *Microbiology* **2008**, *154*, 2060–2069. [CrossRef]
9. Done, H.Y.; Venkatesan, A.K.; Halden, R.U. Does the Recent Growth of Aquaculture Create Antibiotic Resistance Threats Different from those Associated with Land Animal Production in Agriculture? *AAPS J.* **2015**, *17*, 513–524. [CrossRef]
10. Watts, J.E.M.; Schreier, H.J.; Lanska, L.; Hale, M.S. The Rising Tide of Antimicrobial Resistance in Aquaculture: Sources, Sinks and Solutions. *Mar. Drugs* **2017**, *15*, 158. [CrossRef]
11. Yu, J.E.; Cho, M.Y.; Kim, J.-W.; Kang, H.Y. Large antibiotic-resistance plasmid of Edwardsiella tarda contributes to virulence in fish. *Microb. Pathog.* **2012**, *52*, 259–266. [CrossRef]
12. Roberts, M.C. Update on acquired tetracycline resistance genes. *FEMS Microbiol. Lett.* **2005**, *245*, 195–203. [CrossRef] [PubMed]
13. Aslam, B.; Wang, W.; Arshad, M.I.; Khurshid, M.; Muzammil, S.; Nisar, M.A.; Alvi, R.F.; Aslam, M.A.; Qamar, M.U.; Salamat, M.K.F.; et al. Antibiotic resistance: A rundown of a global crisis. *Infect. Drug Resist.* **2018**, *11*, 1645–1658. [CrossRef] [PubMed]
14. Oishi, K.; Morise, M.; Vo, L.K.; Tran, N.T.; Sahashi, D.; Ueda-Wakamatsu, R.; Nishimura, W.; Komatsu, M.; Shiozaki, K. Host lactosylceramide enhances Edwardsiella tarda infection. *Cell Microbiol.* **2021**, *23*, e13365. [CrossRef] [PubMed]
15. Leal, Y.; Velazquez, J.; Hernandez, L.; Swain, J.K.; Rodríguez, A.R.; Martínez, R.; García, C.; Ramos, Y.; Estrada, M.P.; Carpio, Y. Promiscuous T cell epitopes boosts specific IgM immune response against a P0 peptide antigen from sea lice in different teleost species. *Fish Shellfish Immunol.* **2019**, *92*, 322–330. [CrossRef]
16. Ashfaq, H.; Soliman, H.; Fajmann, S.; Sexl, V.; El-Matbouli, M.; Saleh, M. Kinetics of CD4-1+ lymphocytes in brown trout after exposure to viral haemorrhagic septicaemia virus. *J. Fish Dis.* **2021**, *44*, 1553–1562. [CrossRef]
17. Nakanishi, T.; Fischer, U.; Dijkstra, J.; Hasegawa, S.; Somamoto, T.; Okamoto, N.; Ototake, M. Cytotoxic T cell function in fish. *Dev. Comp. Immunol.* **2002**, *26*, 131–139. [CrossRef]
18. Adams, A. Progress, challenges, and opportunities in fish vaccine development. *Fish Shellfish Immunol.* **2019**, *90*, 210–214. [CrossRef]
19. Grimholt, U. MHC and Evolution in Teleosts. *Biology* **2016**, *5*, 6. [CrossRef]
20. Dijkstra, J.M.; Grimholt, U.; Leong, J.; Koop, B.F.; Hashimoto, K. Comprehensive analysis of MHC class II genes in teleost fish genomes reveals dispensability of the peptide-loading DM system in a large part of vertebrates. *BMC Evol. Biol.* **2013**, *13*, 260. [CrossRef]
21. Yamaguchi, T.; Dijkstra, J.M. Major Histocompatibility Complex (MHC) Genes and Disease Resistance in Fish. *Cells* **2019**, *8*, 378. [CrossRef]
22. Stosik, M.; Tokarz-Deptuła, B.; Deptuła, W. Major Histocompatibility Complex in Osteichthyes. *J. Vet. Res.* **2020**, *64*, 127–136. [CrossRef] [PubMed]
23. Bolnick, D.I.; Snowberg, L.; Stutz, W.; Caporaso, G.; Lauber, C.; Knight, R.; Lauber, C.; Caporaso, J.G. Major Histocompatibility Complex class IIb polymorphism influences gut microbiota composition and diversity. *Mol. Ecol.* **2014**, *23*, 4831–4845. [CrossRef] [PubMed]
24. Marana, M.H.; Jørgensen, L.V.G.; Skov, J.; Chettri, J.K.; Holm Mattsson, A.; Dalsgaard, I.; Kania, W.P.; Buchmann, K. Subunit vaccine candidates against Aeromonas salmonicida in rainbow trout Oncorhynchus mykiss. *PLoS ONE* **2017**, *12*, e0171944. [CrossRef] [PubMed]
25. Mahendran, R.; Jeyabaskar, S.; Michael, R.D.; Paul, A.V.; Sitharaman, G. Computer-aided vaccine designing approach against fish pathogens Edwardsiella tarda and Flavobacterium columnare using bioinformatics softwares. *Drug Des. Dev. Ther.* **2016**, *10*, 1703–1714. [CrossRef] [PubMed]
26. Pereira, U.P.; Soares, S.; Blom, J.; Leal, C.; Ramos, R.; Guimarães, L.C.; Oliveira, L.; Almeida, S.; Hassan, S.; Santos, A.; et al. In silico prediction of conserved vaccine targets in Streptococcus agalactiae strains isolated from fish, cattle, and human samples. *Genet. Mol. Res.* **2013**, *12*, 2902–2912. [CrossRef] [PubMed]

27. Pumchan, A.; Krobthong, S.; Roytrakul, S.; Sawatdichaikul, O.; Kondo, H.; Hirono, I.; Areechon, N.; Unajak, S. Novel Chimeric Multiepitope Vaccine for Streptococcosis Disease in Nile Tilapia (*Oreochromis niloticus* Linn.). *Sci. Rep.* **2020**, *10*, 603. [CrossRef] [PubMed]
28. Islam, S.I.; Mou, M.J.; Sanjida, S.; Tariq, M.; Nasir, S.; Mahfuj, S. Designing a novel mRNA vaccine against *Vibrio harveyi* infection in fish: An immunoinformatics approach. *Genom. Inform.* **2022**, *20*, e11. [CrossRef]
29. Islam, S.I.; Mou, M.J.; Sanjida, S. Application of reverse vaccinology for designing of an mRNA vaccine against re-emerging marine birnavirus affecting fish species. *Inform. Med. Unlocked* **2022**, *30*, 100948. [CrossRef]
30. Hansson, M.; Nygren, P.-A.K.; Ståhl, S. Design and production of recombinant subunit vaccines. *Biotechnol. Appl. Biochem.* **2000**, *32*, 95–107. [CrossRef]
31. Madonia, A.; Melchiorri, C.; Bonamano, S.; Marcelli, M.; Bulfon, C.; Castiglione, F.; Galeotti, M.; Volpatti, D.; Mosca, F.; Tiscar, P.-G.; et al. Computational modeling of the immune system of the fish for a more effective vaccination in aquaculture. *Bioinformatics* **2017**, *33*, 3065–3071. [CrossRef]
32. Joshi, A.; Pathak, D.C.; Mannan, M.A.-U.; Kaushik, V. In-silico designing of an epitope-based vaccine against the seven banded grouper nervous necrosis virus affecting fish species. *Netw. Model. Anal. Health Inform. Bioinform.* **2021**, *10*, 37. [CrossRef] [PubMed]
33. Sherry, S.T.; Ward, M.-H.; Kholodov, M.; Baker, J.; Phan, L.; Smigielski, E.M.; Sirotkin, K. dbSNP: The NCBI database of genetic variation. *Nucleic Acids Res.* **2001**, *29*, 308–311. [CrossRef] [PubMed]
34. Rahman, N.; Ajmal, A.; Ali, F.; Rastrelli, L. Core proteome mediated therapeutic target mining and multi-epitope vaccine design for *Helicobacter pylori*. *Genomics* **2020**, *112*, 3473–3483. [CrossRef] [PubMed]
35. Sanober, G.; Ahmad, S.; Azam, S. Identification of plausible drug targets by investigating the druggable genome of MDR *Staphylococcus epidermidis*. *Gene Rep.* **2017**, *7*, 147–153. [CrossRef]
36. Rédei, G. NCBI (National Center for Biotechnology Information) Encyclopedia of Genetics, Genomics, Proteomics and Informatics. 2008. Available online: https://www.ncbi.nlm.nih.gov/ (accessed on 1 June 2022).
37. Shenoy, P.; Vin, H. Cello: A Disk Scheduling Framework for Next-Generation Operating Systems *. *Real-Time Syst.* **2002**, *22*, 9–48. [CrossRef]
38. Chen, L.; Yang, J.; Yu, J.; Yao, Z.; Sun, L.; Shen, Y.; Jin, Q. VFDB: A reference database for bacterial virulence factors. *Nucleic Acids Res.* **2005**, *33*, D325–D328. [CrossRef] [PubMed]
39. Krogh, A.; Larsson, B.; von Heijne, G.; Sonnhammer, E.L. Predicting Transmembrane Protein Topology with a Hidden Markov Model: Application to Complete Genomes. *J. Mol. Biol.* **2001**, *305*, 567–580. [CrossRef]
40. Meunier, M.; Guyard-Nicodème, M.; Hirchaud, E.; Parra, A.; Chemaly, M.; Dory, D. Identification of Novel Vaccine Candidates against Campylobacter through Reverse Vaccinology. *J. Immunol. Res.* **2016**, *2016*, 5715790. [CrossRef]
41. Doytchinova, I.A.; Flower, D.R. VaxiJen: A server for prediction of protective antigens, tumour antigens and subunit vaccines. *BMC Bioinform.* **2007**, *8*, 4. [CrossRef]
42. Garg, V.K.; Avashthi, H.; Tiwari, A.; Jain, P.A.; Ramkete, P.W.; Kayastha, A.M.; Singh, V.K. MFPPI-Multi FASTA ProtParam Interface. *Bioinformation* **2016**, *12*, 74–77. [CrossRef]
43. Dimitrov, I.; Bangov, I.; Flower, D.R.; Doytchinova, I. AllerTOP v.2—A server for in silico prediction of allergens. *J. Mol. Model.* **2014**, *20*, 2278. [CrossRef] [PubMed]
44. Farhood, B.; Najafi, M.; Mortezaee, K. CD8 + cytotoxic T lymphocytes in cancer immunotherapy: A review. *J. Cell. Physiol.* **2018**, *234*, 8509–8521. [CrossRef] [PubMed]
45. Bhasin, M.; Raghava, G.P. Prediction of CTL epitopes using QM, SVM, and ANN techniques. *Vaccine* **2004**, *22*, 3195–3204. [CrossRef]
46. He, Y.; Xiang, Z.; Mobley, H.L. Vaxign: The first web-based vaccine design program for reverse vaccinology and applications for vaccine development. *J. Biomed. Biotechnol.* **2010**, *2010*, 297505. [CrossRef]
47. Calis, J.J.; Maybeno, M.; Greenbaum, J.A.; Weiskopf, D.; De Silva, A.D.; Sette, A.; Keşmir, C.; Peters, B. Properties of MHC class I presented peptides that enhance immunogenicity. *PLoS Comput. Biol.* **2013**, *9*, e1003266. [CrossRef] [PubMed]
48. Gupta, S.; Kapoor, P.; Chaudhary, K.; Gautam, A.; Kumar, R.; Open Source Drug Discovery Consortium; Raghava, G.P. In silico approach for predicting the toxicity of peptides and proteins. *PLoS ONE* **2013**, *8*, e73957. [CrossRef] [PubMed]
49. Dimitrov, I.; Flower, D.R.; Doytchinova, I. AllerTOP—A server for in silico prediction of allergens. *BMC Bioinform.* **2013**, *14* (Suppl. S6), S4. [CrossRef]
50. Nain, Z.; Abdullah, F.; Rahman, M.M.; Karim, M.M.; Khan, S.A.; Bin Sayed, S.; Mahmud, S.; Rahman, S.M.R.; Sheam, M.; Haque, Z.; et al. Proteome-wide screening for designing a multi-epitope vaccine against emerging pathogen *Elizabethkingia anophelis* using immunoinformatic approaches. *J. Biomol. Struct. Dyn.* **2020**, *38*, 4850–4867. [CrossRef]
51. Manavalan, B.; Govindaraj, R.G.; Shin, T.H.; Kim, M.O.; Lee, G. iBCE-EL: A New Ensemble Learning Framework for Improved Linear B-Cell Epitope Prediction. *Front. Immunol.* **2018**, *9*, 1695. [CrossRef]
52. Latysheva, N.S.; Babu, M.M. Discovering and understanding oncogenic gene fusions through data-intensive computational approaches. *Nucleic Acids Res.* **2016**, *44*, 4487–4503. [CrossRef]
53. Chen, X.; Zaro, J.L.; Shen, W.C. Fusion protein linkers: Property, design, and functionality. *Adv. Drug Deliv. Rev.* **2013**, *65*, 1357–1369. [CrossRef] [PubMed]

54. Trott, O.; Olson, A.J. AutoDock Vina: Improving the speed and accuracy of docking with a new scoring function, efficient optimization, and multithreading. *J. Comput. Chem.* **2010**, *31*, 455–461. [CrossRef] [PubMed]
55. Unajak, S.; Pumchan, A.; Roytrakul, S.; Sawatdichaikul, O.; Areechon, N. Novel Vaccine Development for Fish Culture Based on the Multiepitope Concept. *Methods Mol. Biol.* **2022**, *2411*, 219–240. [PubMed]
56. Dorosti, H.; Eslami, M.; Negahdaripour, M.; Ghoshoon, M.B.; Gholami, A.; Heidari, R.; Dehshahri, A.; Erfani, N.; Nezafat, N.; Ghasemi, Y. Vaccinomics approach for developing multi-epitope peptide pneumococcal vaccine. *J. Biomol. Struct. Dyn.* **2019**, *37*, 3524–3535. [CrossRef]
57. Abdellrazeq, G.S.; Fry, L.M.; Elnaggar, M.M.; Bannantine, J.P.; Schneider, D.A.; Chamberlin, W.M.; Mahmoud, A.H.; Park, K.-T.; Hulubei, V.; Davis, W.C. Simultaneous cognate epitope recognition by bovine CD4 and CD8 T cells is essential for the primary expansion of antigen-specific cytotoxic T-cells following ex vivo stimulation with a candidate *Mycobacterium avium subsp. paratuberculosis* peptide vaccine. *Vaccine* **2020**, *38*, 2016–2025. [CrossRef]
58. Wilkins, M.R.; Gasteiger, E.; Bairoch, A.; Sanchez, J.C.; Williams, K.L.; Appel, R.D.; Hochstrasser, D.F. Protein Identification and Analysis Tools in the ExPASy Server. In *2-D Proteome Analysis Protocols. Methods in Molecular Biology*; Humana Press: Totowa, NJ, USA, 1999; Volume 112, pp. 531–552.
59. Buchan, D.W.; Minneci, F.; Nugent, T.C.O.; Bryson, K.; Jones, D.T. Scalable web services for the PSIPRED Protein Analysis Workbench. *Nucleic Acids Res.* **2013**, *41*, W349–W357. [CrossRef]
60. Geourjon, C.; Deléage, G. SOPMA: Significant improvements in protein secondary structure prediction by consensus prediction from multiple alignments. *Comput. Appl. Biosci.* **1995**, *11*, 681–684. [CrossRef]
61. Xu, J.; McPartlon, M.; Li, J. Improved protein structure prediction by deep learning irrespective of co-evolution information. *Nat. Mach. Intell.* **2021**, *3*, 601–609. [CrossRef]
62. Nugent, T.; Cozzetto, D.; Jones, D.T. Evaluation of predictions in the CASP10 model refinement category. *Proteins* **2014**, *82* (Suppl. S2), 98–111. [CrossRef]
63. DeLano, W.L. PyMOL: An Open-Source Molecular Graphics Tool. *CCP4 Newsl. Protein Cryst.* **2002**, *40*, 82–92.
64. Wiederstein, M.; Sippl, M.J. ProSA-web: Interactive web service for the recognition of errors in three-dimensional structures of proteins. *Nucleic Acids Res.* **2007**, *35*, W407–W410. [CrossRef] [PubMed]
65. Craig, D.B.; Dombkowski, A.A. Disulfide by Design 2.0: A web-based tool for disulfide engineering in proteins. *BMC Bioinform.* **2013**, *14*, 346. [CrossRef] [PubMed]
66. Kozakov, D.; Hall, D.R.; Xia, B.; Porter, K.A.; Padhorny, D.; Yueh, C.; Beglov, D.; Vajda, S. The ClusPro web server for protein-protein docking. *Nat. Protoc.* **2017**, *12*, 255–278. [CrossRef] [PubMed]
67. Pokhrel, S.; Bouback, T.A.; Samad, A.; Nur, S.M.; Alam, R.; Abdullah-Al-Mamun, M.; Nain, Z.; Imon, R.R.; Talukder, M.E.K.; Tareq, M.M.I.; et al. Spike protein recognizer receptor ACE2 targeted identification of potential natural antiviral drug candidates against SARS-CoV-2. *Int. J. Biol. Macromol.* **2021**, *191*, 1114–1125. [CrossRef] [PubMed]
68. Krieger, E.; Vriend, G. New ways to boost molecular dynamics simulations. *J. Comput. Chem.* **2015**, *36*, 996–1007. [CrossRef]
69. Krieger, E.; Darden, T.; Nabuurs, S.B.; Finkelstein, A.; Vriend, G. Making optimal use of empirical energy functions: Force-field parameterization in crystal space. *Proteins Struct. Funct. Bioinform.* **2004**, *57*, 678–683. [CrossRef]
70. Desai, V.H.; Kumar, S.P.; Pandya, H.A.; Solanki, H. Receptor-Guided De Novo Design of Dengue Envelope Protein Inhibitors. *Appl. Biochem. Biotechnol.* **2015**, *177*, 861–878. [CrossRef]
71. Rapin, N.; Lund, O.; Bernaschi, M.; Castiglione, F. Computational immunology meets bioinformatics: The use of prediction tools for molecular binding in the simulation of the immune system. *PLoS ONE* **2010**, *5*, e9862. [CrossRef]
72. Castiglione, F.; Mantile, F.; De Berardinis, P.; Prisco, A. How the interval between prime and boost injection affects the immune response in a computational model of the immune system. *Comput. Math. Methods Med.* **2012**, *2012*, 842329. [CrossRef]
73. Grote, A.; Hiller, K.; Scheer, M.; Münch, R.; Nörtemann, B.; Hempel, D.C.; Jahn, D. JCat: A novel tool to adapt codon usage of a target gene to its potential expression host. *Nucleic Acids Res.* **2005**, *33*, W526–W531. [CrossRef]
74. Goldberg, M.F.; Roeske, E.K.; Ward, L.N.; Pengo, T.; Dileepan, T.; Kotov, D.I.; Jenkins, M.K. Salmonella Persist in Activated Macrophages in T Cell-Sparse Granulomas but Are Contained by Surrounding CXCR3 Ligand-Positioned Th1 Cells. *Immunity* **2018**, *49*, 1090–1102.e7. [CrossRef] [PubMed]
75. Hassan, A.; Naz, A.; Obaid, A.; Paracha, R.Z.; Naz, K.; Awan, F.M.; Muhammad, S.A.; Janjua, H.A.; Ahmad, J.; Ali, A. Pangenome and immuno-proteomics analysis of *Acinetobacter baumannii* strains revealed the core peptide vaccine targets. *BMC Genom.* **2016**, *17*, 732. [CrossRef] [PubMed]
76. Sakharkar, K.R.; Sakharkar, M.K.; Chow, V.T. A novel genomics approach for the identification of drug targets in pathogens, with special reference to Pseudomonas aeruginosa. *Silico Biol.* **2004**, *4*, 355–360.
77. Li, W.; Joshi, M.D.; Singhania, S.; Ramsey, K.H.; Murthy, A.K. Peptide Vaccine: Progress and Challenges. *Vaccines* **2014**, *2*, 515–536. [CrossRef] [PubMed]
78. Bol, K.F.; Aarntzen, E.H.J.G.; Pots, J.M.; Nordkamp, M.A.M.O.; Van De Rakt, M.W.M.M.; Scharenborg, N.M.; De Boer, A.J.; Van Oorschot, T.G.M.; Croockewit, S.A.J.; Blokx, W.A.M.; et al. Prophylactic vaccines are potent activators of monocyte-derived dendritic cells and drive effective anti-tumor responses in melanoma patients at the cost of toxicity. *Cancer Immunol. Immunoth.* **2016**, *65*, 327–339. [CrossRef]

79. Shamriz, S.; Ofoghi, H.; Moazami, N. Effect of linker length and residues on the structure and stability of a fusion protein with malaria vaccine application. *Comput. Biol. Med.* **2016**, *76*, 24–29. [CrossRef]
80. Bonam, S.R.; Partidos, C.D.; Halmuthur, S.K.M.; Muller, S. An Overview of Novel Adjuvants Designed for Improving Vaccine Efficacy. *Trends Pharmacol. Sci.* **2017**, *38*, 771–793. [CrossRef]
81. Khatoon, N.; Pandey, R.K.; Prajapati, V.K. Exploring Leishmania secretory proteins to design B and T cell multi-epitope subunit vaccine using immunoinformatics approach. *Sci. Rep.* **2017**, *7*, 8285. [CrossRef]